

# Conserved sandpile with a variable height restriction

Vanuildo de Carvalho and Álvaro de Almeida Caparica\*

*Instituto de Física, Universidade Federal de Goiás,  
C.P.131, 74.001-970, Goiânia (GO), Brazil*

Ronald Dickman

*Departamento de Física and National Institute  
of Science and Technology for Complex Systems,  
ICEx, Universidade Federal de Minas Gerais,  
Caixa Postal 702, 30161-970 Belo Horizonte, MG, Brazil*

## Abstract

We study a restricted-height version of the one-dimensional Oslo sandpile with conserved density, using periodic boundary conditions. Each site has a limiting height which can be either two or three. When a site reaches its limiting height it becomes active and may topple, losing two particles, which move randomly to nearest-neighbor sites. After a site topples it is randomly assigned a new limiting height. We study the model using mean-field theory and Monte Carlo simulation, focusing on the quasi-stationary state, in which the number of active sites fluctuates about a stationary value. Using finite-size scaling analysis, we determine the critical particle density and associated critical exponents.

PACS numbers:

Keywords: SOC, mean-field theory, computer simulation

---

\*Electronic address: caparica@if.ufg.br

## I. INTRODUCTION

Sandpile models are paradigmatic examples of self-organized criticality (SOC) [1, 2], a control mechanism that forces a system with an absorbing-state phase transition to its critical point [3–5], without explicit tuning of control parameters [6]. SOC in a slowly driven sandpile corresponds to an absorbing-state phase transition in a model with the same local dynamics, but a fixed number of particles [3, 7–11], so-called *conserved sandpiles* [10, 12–14]. Absorbing-state phase transitions arise in the context of spatial stochastic models, and correspond to a transition between an active, fluctuating phase, and an absorbing one, which allows no escape [24, 25, 27].

Sandpile models with probabilistic toppling rules, typified by the Manna model [15, 16], are commonly designated as *stochastic sandpiles*; their study has been central to establishing the connection between SOC and absorbing-state phase transitions. An important stochastic model is the Oslo model [17], inspired by experimental studies on rice piles. In this work we study a conserved version of the Oslo model, characterizing its absorbing-state critical point.

An inconvenient feature of many sandpile models is the absence of an upper bound on the number of particles that may occupy a given site, which complicates theoretical approaches such as  $n$ -site approximations or continuum descriptions. This motivated the study of *restricted sandpiles* [18]. In the present work we impose a height restriction on the conserved Oslo model. Since the symmetries and conserved quantities of the restricted and unrestricted models are the same, one expects, on the basis of experience with critical phenomena both in and out of equilibrium, that the models belong to the same universality class, as is indeed borne out for conserved versions of the Manna model [19–21]. The symmetries here are limited to spatial translation and inversion, while the conservation law is that of particle number. This universality class has come to be known as the conserved directed percolation (CDP) class. Recently it was suggested that the critical behavior of conserved stochastic sandpiles in fact belongs to the (nonconserved) directed percolation class [22], but further studies are required to verify this assertion.

The remainder of this paper is organized as follows: In Section II we describe the model and in Section III develop a one-site mean-field approximation. Our numerical

results are reported in Section IV and in Section V we present our conclusions.

## II. MODEL

We study a restricted sandpile model with a variable height limit, defined on a lattice of  $N_{site} = L^d$  sites, where  $d$  is the dimension of space. The configuration is specified by the particle numbers  $z_i$  ( $i = 1, \dots, N_{site}$ ) at each site. Each site has a *critical height*  $c_i \in \{2, 3\}$ , with equal probability, such that  $z_i \leq c_i$ . A site with  $z_i = c_i$  is said to be *active*. Any configuration devoid of active sites is *absorbing*, i.e., it admits no escape. The dynamics of the model proceeds via *toppling* of active sites; each active site has a rate of unity to topple. (By a "rate of unity" we mean that the time unit is chosen such that if there are currently  $N_A$  active sites, then the time increment associated with the next toppling is  $1/N_A$ .) In a continuous-time (sequential) dynamics, each active site has the same probability of being the next to topple. When a site, say  $i$ , topples, two particles are transferred from  $i$  to sites  $j$  and  $j'$ , nearest neighbors of  $i$ . The two sites are chosen at random, independently, from the set of nearest neighbors, and so are not necessarily distinct; we refer to this procedure as an *independent* toppling rule. Due to the height restriction, any particle transfer that would result in a target site  $j$  having  $z_j > c_j$  is rejected. (This means that the configuration  $z_i = c_i, \forall i$  is also absorbing, since no particles can be transferred. The particle densities of interest in this study, however, remain far below the density associated with this configuration.) When site  $i$  loses a particle or particles due to toppling, a new limiting height  $c_i$  is selected, equal to 2 or 3, each with probability  $1/2$ . Thus the dynamics has three stochastic elements: (1) the choice of the next site to topple; (2) the choice of target sites  $j$  and  $j'$  for particle transfers; (3) the choice of the new limiting height after a site topples.

In practice the next site to topple is selected at random from a list of currently active sites, which must naturally be updated following each toppling event. The time increment associated with each toppling (whether particles are transferred or not) is  $\Delta t = 1/N_a$ , with  $N_a$  the number of active sites immediately prior to the event.

### III. MEAN-FIELD THEORY

The primary aim of the mean-field analysis is to obtain a preliminary idea of the phase diagram and (assuming the latter possesses a phase transition), an order of magnitude estimate of the critical point. We consider the simplest mean-field approach, known as the one-site approximation. At this level of approximation, there are seven possible states ( $i|j$ ) for a given site, where  $i = 0, 1, \dots, j$  represents the occupation number and  $j = 2, 3$  denotes the limiting height, with associated probabilities denoted by  $P_{ij}$ . Taking into account the conditions of normalization

$$\sum_{j=2}^3 \sum_{i=0}^j P_{ij} = 1, \quad (1)$$

and of fixed density,

$$\sum_{j=2}^3 \sum_{i=0}^j iP_{ij} = \zeta, \quad (2)$$

there are only five independent variables at this level.

We begin the analysis by listing the possible transitions between states ( $i|j$ ) in Fig. 1. Each transition (at a given site, called the *central site* in this discussion), requires a specific configuration at the central site and at one or both of its nearest neighbors, and a certain redistribution of particles from the toppling site. (The local configuration and the choice of target sites,  $j$  and  $j'$ , in the particle redistribution are statistically independent events.) In the one-site approximation, joint probabilities involving two or more sites are factorized. Denoting a joint two-site probability by  $P_{ij|kl}$ , the one-site approximation uses the replacement  $P_{ij|kl} \rightarrow P_{ij}P_{kl}$ , and similarly for three-site probabilities.

To illustrate how the rates associated with these transitions are calculated, we discuss some examples. Consider first the transition  $(0|2) \rightarrow (1|2)$ . The initial configuration must be either  $(02|22)$  or  $(03|23)$ , that is, the central site must be vacant, have  $z_c = 2$ , and have an active neighbor. When the latter topples, exactly one particle must migrate to the central site. On a hypercubic lattice in  $d$  dimensions, each site has  $2d$  nearest neighbors. Since the probability of exactly one particle

		FROM:						
		(0 2)	(0 3)	(1 2)	(1 3)	(2 2)	(2 3)	(3 3)
TO:	(0 2)		X	X	X		X	X
	(0 3)	X		X	X		X	X
	(1 2)		X		X		X	
	(1 3)	X		X		X		
	(2 2)		X		X		X	
	(2 3)	X		X		X		
	(3 3)	X	X	X		X		

FIG. 1: Transitions between states of a single site. Transitions marked “X” are impossible and those ones related to diagonal elements are irrelevant.

jumping to the central site is  $2(1/2d)[1 - (1/2d)]$ , the rate (per site) of transitions of the kind  $(0|2) \rightarrow (1|2)$  is

$$2d \frac{2d-1}{2d^2} P_{02}(P_{22} + P_{33}), \quad (3)$$

where the factor  $2d$  represents the number of nearest neighbors.

Consider next the transition  $(2|2) \rightarrow (0|2)$ , which can occur via two mutually exclusive paths. In one, both particles liberated when the central site topples attempt to migrate to the same neighbor, an event having probability  $1/4d^2$ . In order for both particles to actually migrate, the difference  $z_c - z$  at the target site must be greater than one. Thus the initial configurations for which this transition may occur are  $(00|23)$ ,  $(02|32)$ , and  $(12|32)$ . The transition rate for this path is

$$\frac{1}{2} 2d \frac{1}{4d^2} P_{22}(P_{02} + P_{03} + P_{13}), \quad (4)$$

where the factor  $1/2$  represents the probability that the limiting height retains the value of 2 following the toppling event. In the other path, the two particles migrate

to distinct neighbors of the central site. The configurations that allow this transition to occur are  $(2^\dagger 22^\dagger | 222)$ ,  $(2^\dagger 23^\dagger | 223)$ , and  $(3^\dagger 23^\dagger | 323)$ , where  $2^\dagger$  and  $3^\dagger$  denote, respectively, sites with  $z < 2$  and  $z < 3$ . Thus the transition rate for this path is

$$\frac{2d-1}{4d} P_{22} (P_{2^\dagger 2} + P_{3^\dagger 3})^2. \quad (5)$$

Evaluating the rates of the remaining transitions, we find the equations that govern the probabilities  $P_{i,j}$  at this level of approximation. The equations for the  $P_{ij}$  are

$$\begin{aligned} \frac{dP_{02}(t)}{dt} = & \frac{1}{4d} P_{22} (P_{02} + P_{03} + P_{13}) + \frac{2d-1}{4d} P_{22} (P_{2^\dagger 2} + P_{3^\dagger 3})^2 - \frac{4d-1}{2d} P_{02} \\ & \times (P_{22} + P_{33}), \end{aligned} \quad (6)$$

$$\begin{aligned} \frac{dP_{03}(t)}{dt} = & \frac{1}{4d} P_{22} (P_{02} + P_{03} + P_{13}) + \frac{2d-1}{4d} P_{22} (P_{2^\dagger 2} + P_{3^\dagger 3})^2 - \frac{4d-1}{2d} P_{03} \\ & \times (P_{22} + P_{33}), \end{aligned} \quad (7)$$

$$\begin{aligned} \frac{dP_{23}(t)}{dt} = & \frac{1}{2d} [P_{03} + 2(2d-1)P_{13} - (4d-1)P_{23}] (P_{22} + P_{33}) + \frac{1}{4d} [1 + 2(2d-1) \\ & \times (P_{22} + P_{33})] (P_{12} + P_{23}) P_{33}, \end{aligned} \quad (8)$$

$$\begin{aligned} \frac{dP_{12}(t)}{dt} = & \left( \frac{2d-1}{2d} P_{02} - \frac{4d-1}{2d} P_{12} \right) (P_{22} + P_{33}) + \frac{1}{4d} [1 + 2(2d-1)(P_{22} + P_{33})] \\ & \times P_{22} (P_{12} + P_{23}) + \frac{1}{4d} [P_{02} + P_{03} + P_{13} + (2d-1)(P_{2^\dagger 2} + P_{3^\dagger 3})^2] P_{33}, \end{aligned} \quad (9)$$

$$\begin{aligned} \frac{dP_{13}(t)}{dt} = & \left( \frac{2d-1}{2d} P_{03} - \frac{4d-1}{2d} P_{13} \right) (P_{22} + P_{33}) + \frac{1}{4d} [1 + 2(2d-1)(P_{22} + P_{33})] \\ & \times P_{22} (P_{12} + P_{23}) + \frac{1}{4d} [P_{02} + P_{03} + P_{13} + (2d-1)(P_{2^\dagger 2} + P_{3^\dagger 3})^2] P_{33}, \end{aligned} \quad (10)$$

$$\begin{aligned} \frac{dP_{22}(t)}{dt} = & \frac{1}{2d} [P_{02} + (4d-1)P_{12}] (P_{22} + P_{33}) + \frac{1}{4d} [1 + 2(2d-1)(P_{22} + P_{33})] \\ & \times P_{33} (P_{12} + P_{23}) - \frac{1}{2d} [P_{02} + P_{03} + P_{13} + (2d-1)(P_{2^\dagger 2} + P_{3^\dagger 3})^2] P_{22} \\ & + \frac{1}{2d} [1 + 2(2d-1)(P_{22} + P_{33})] P_{22} (P_{12} + P_{23}), \end{aligned} \quad (11)$$

$$\begin{aligned} \frac{dP_{33}(t)}{dt} = & \frac{1}{2d} [P_{13} + (4d-1)P_{23}] (P_{22} + P_{33}) - \frac{1}{2d} [P_{02} + P_{03} + P_{13}] P_{33} \\ & + \frac{2d-1}{2d} (P_{2^\dagger 2} + P_{3^\dagger 3})^2 P_{33} - \frac{1}{2d} [1 + 2(2d-1)(P_{22} + P_{33})] P_{33} \\ & \times (P_{12} + P_{23}). \end{aligned} \quad (12)$$

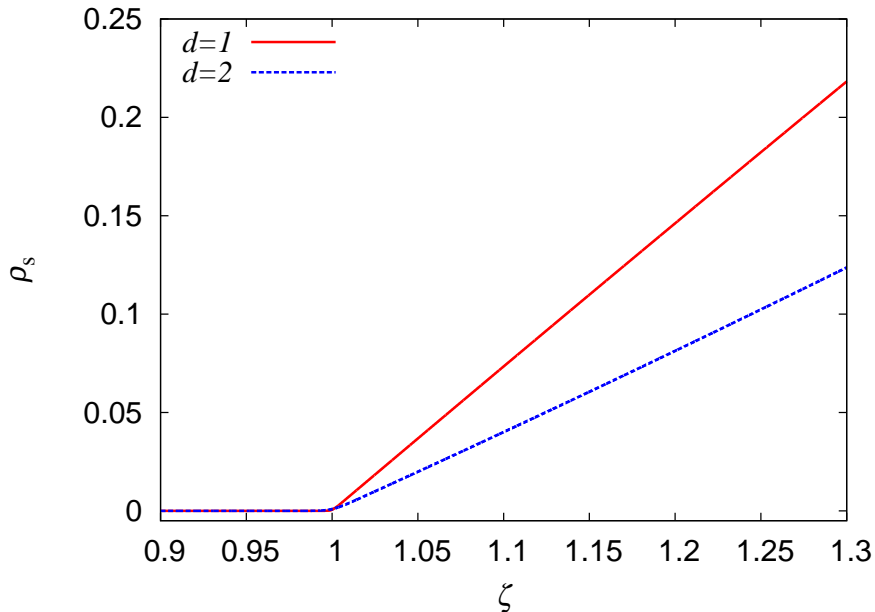


FIG. 2: Stationary order parameter  $\rho_s$  versus density  $\zeta$ , in the one-site approximation, for  $d = 1$  and  $d = 2$ .

Solution of the above equations is performed numerically. We note that in light of the constraints expressed in Eqs. (1) and (2), we have only five independent equations. We also take advantage of the following symmetry: in the mean-field approximation, if  $P_{02} = P_{03}$  initially, then this equality continues to hold throughout the evolution. A similar relation holds between  $P_{12}(t)$  and  $P_{13}(t)$ . We therefore obtain a set of three independent differential equations for  $P_{22}(t)$ ,  $P_{23}(t)$  e  $P_{33}(t)$ , which are readily integrated using a fourth-order Runge-Kutta scheme [23]. We define the order parameter as the fraction of active sites,

$$\rho(t) = P_{22}(t) + P_{33}(t). \quad (13)$$

Numerical integration reveals that in one and two dimensions,  $\rho(t) \rightarrow 0$  as  $t \rightarrow \infty$  for particle densities  $\zeta \leq 1$ , while for higher densities it attains a nonzero stationary value  $\rho_s$  (see Fig. 2), which grows continuously with  $\zeta - 1$ . Thus in the one-site approximation, the model exhibits a continuous phase transition between an active and an absorbing state. Such a continuous absorbing-state phase transition is familiar from studies of the contact process [24], and of conserved stochastic sandpiles,

among other models. We verify that for  $\zeta \neq 1$ ,  $\rho(t)$  approaches its stationary value exponentially:  $|\rho(t) - \rho_s| \propto \exp(-t/\tau)$ , where the relaxation time  $\tau$  depends on  $\zeta$ , and diverges as  $\zeta \rightarrow \zeta_c = 1$ , following  $\tau \sim 1/|\zeta - \zeta_c|$ , as is typical for mean-field analysis of absorbing-state phase transitions [25]. The one-site approximation yields the critical exponent  $\beta$ , defined via  $\rho_s \sim (\zeta - \zeta_c)^\beta$ , (for  $\zeta > \zeta_c$ ), as  $\beta = 1$  for both  $d = 1$  and  $d = 2$ . This value is expected for mean-field analysis of continuous absorbing-state phase transitions in models that do not possess up-down (or particle-hole) symmetry [25]. The reason is that in the absence of such a symmetry, all powers of the order parameter are allowed in the mean-field equations of motion, so that near the critical point, the terms proportional to  $\rho$  and  $\rho^2$  dominate (that is,  $d\rho/dt \simeq a\rho - b\rho^2$ , with  $a \propto \zeta - \zeta_c$  and  $b > 0$ ), and the stationary value of  $\rho$  is proportional to  $\zeta - \zeta_c$ .

#### IV. SIMULATION

We simulate the restricted sandpile model described above in one dimension using periodic boundaries, on rings of  $L = 500, 1000, 1500$ , and  $2000$  sites. The initial configuration is defined by assigning limiting heights  $z_c = 2$  or  $3$  with equal probabilities, independently, to each site, and then distributing randomly  $N$  particles among the  $L$  sites, avoiding occupancies that exceed the maximum height. The resulting *initial* distribution is statistically homogeneous; the occupations of different sites are essentially independent. Once all  $N$  particles have been inserted, the stochastic dynamics, which, as noted conserves particles, begins. For each system size  $L$ , we study an interval of densities  $\zeta = N/L$ . In all cases, we use  $N_r = 2000$  independent realizations of the process. The maximum time is  $t_m = 5 \times 10^4$  units for  $L = 1000$  and  $t_m = 3 \times 10^5$  for  $L = 2000$ .

To determine the critical behavior of the one-dimensional version of sandpile defined above, we study the time-dependent density of active sites  $\rho(t)$  as well as their survival probability  $P(t)$ . Figure 3 shows the typical simulation behavior for  $\rho(t)$  and  $P(t)$ . We see that  $\rho(t)$  possesses a transient part before reach a well defined stationary value  $\rho_s(\zeta, L)$ , while the survival probability  $P(t) \propto \exp(-t/\tau(\zeta, L))$  has



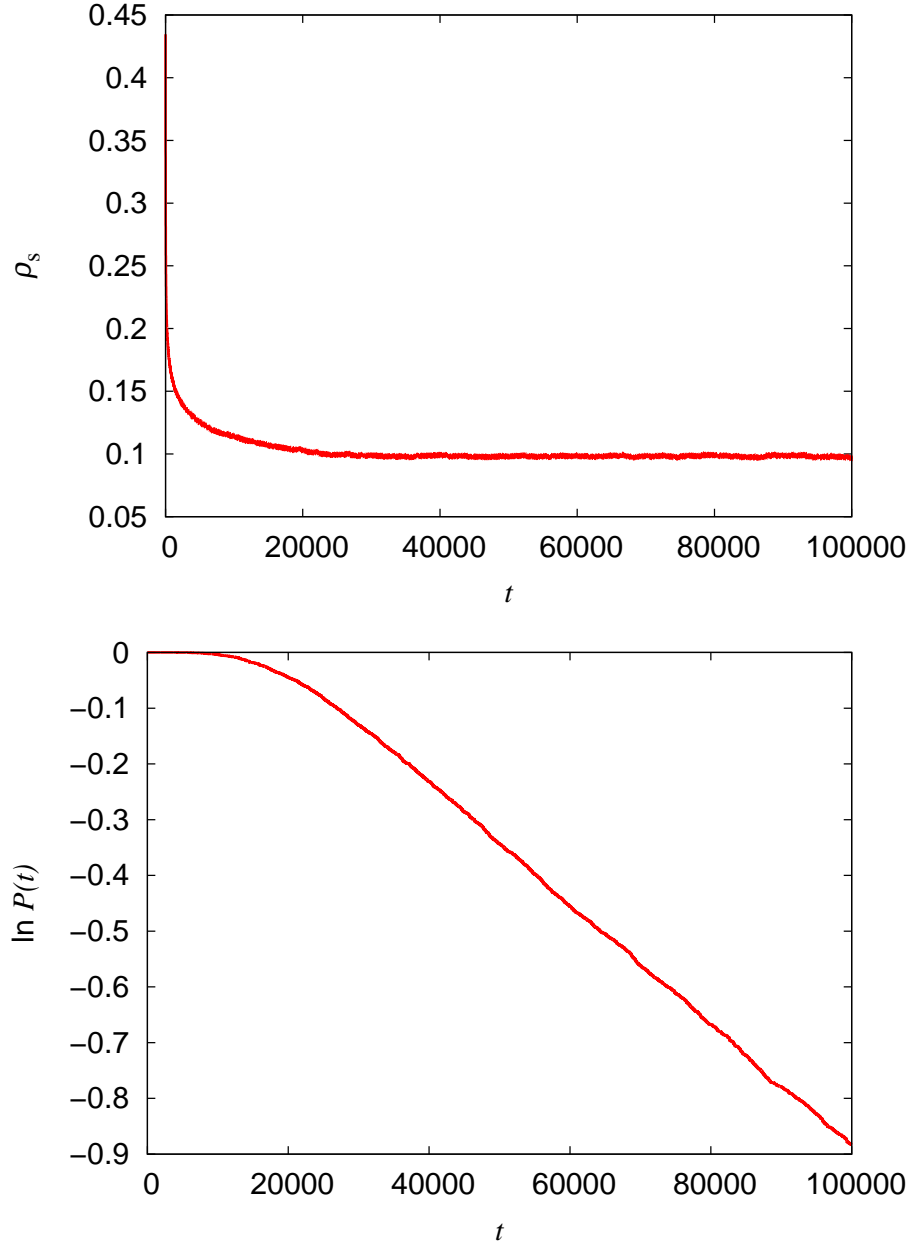


FIG. 3: Simulation: order parameter (upper panel) and survival probability (lower panel) versus time for  $L = 1000$  and particle density  $\zeta = 1.64$ .

an exponential decay. Discarding the initial transient portion of the data the survival time  $\tau(\zeta, L)$  is estimated by the slope of the curve.

In simulations, the particle density  $\zeta$  cannot be varied continuously; for each system size  $L$  it can only be changed in increments of  $1/L$ . To have access to intervals of particle density smaller than  $1/L$ , we follow a method employed in the study of

conserved sandpile models [18] and pair contact process [26]. Initially we determine the stationary average of  $\rho$  for a series of discrete values of the particle density, as shown in Fig. 4. Since it is reasonable to suppose that the resulting points fall on a smooth curve (as is indeed confirmed by the data), we then use quadratic interpolation to estimate  $\rho$  at particle densities that are not accessible for the sizes studied here.

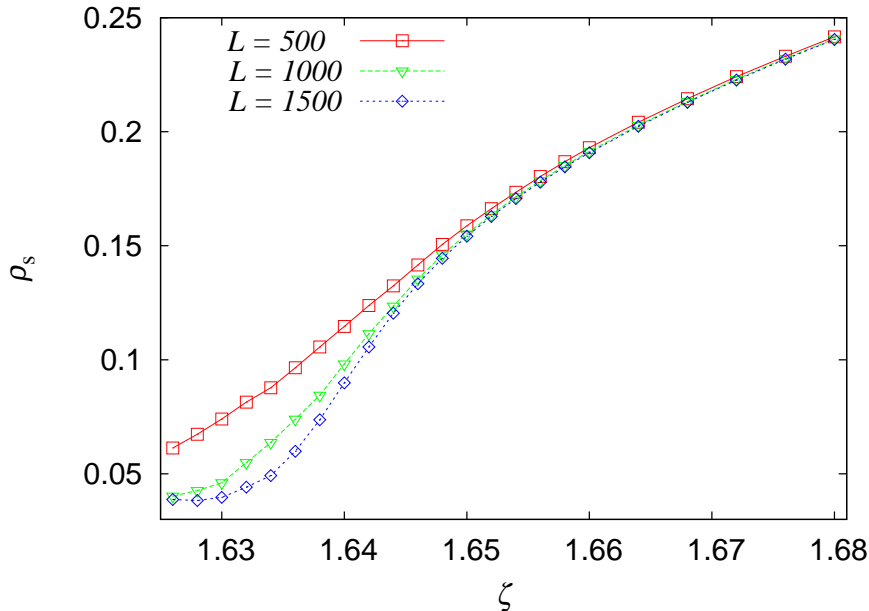


FIG. 4: Simulation: order parameter  $\rho_s$  versus particle density  $\zeta$  for sizes as indicated.

By means the analysis of these data, we obtain the order parameter and the mean survival time as functions of system size for diverse values of the particle density, as shown in Fig. 5. At an absorbing-state phase transition, the critical point of a phase transition is determined by seeking a power-law dependence of the order parameter  $\rho_s$  and the survival time  $\tau$  on the system size  $L$ . These two parameters are governed by

$$\rho_s(\zeta, L) = L^{-\beta/\nu_\perp} \mathbf{C}(L^{1/\nu_\perp} \Delta), \quad (14)$$

$$\tau(\zeta, L) = L^{\nu_\parallel/\nu_\perp} \mathbf{R}(L^{1/\nu_\perp} \Delta), \quad (15)$$

where  $\Delta \equiv \zeta - \zeta_c$  is the distance from criticality and  $\mathbf{C}$  and  $\mathbf{R}$  are finite-size scaling

relations [27]. At the critical point ( $\Delta = 0$ ), we expect  $\rho_s(\zeta_c, L) \sim L^{-\beta/\nu_\perp}$  and  $\tau(\zeta_c, L) \sim L^{\nu_\parallel/\nu_\perp}$ . With this in mind, we can estimate  $\zeta_c$  and  $\beta/\nu_\perp$  from the curve of  $\rho_s(\zeta_c, L)$  that best approximates a straight line when plotted versus  $L$  on log scales.

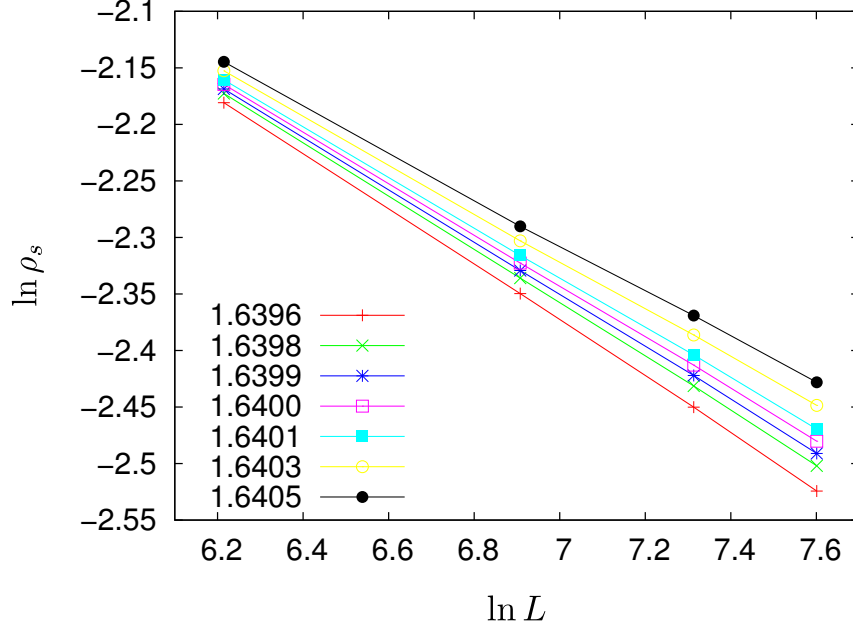


FIG. 5: Stationary order parameter  $\rho_s$  versus system size  $L$  for particle densities  $\zeta$  as indicated.

This analysis yields  $\zeta_c = 1.6400(2)$  and  $\beta/\nu_\perp = 0.227(5)$ , where the figures in parentheses denote the uncertainty in the last significant figure. Analyzing the data for the lifetime  $\tau$  in the same manner, we obtain  $z = \nu_\parallel/\nu_\perp = 1.44(3)$ . (The uncertainties are related to two contributions: one due to the uncertainty of the fit, the other due to the uncertainty in the values of  $\rho_s$  and  $\tau$  for each size  $L$ .) We estimate the critical exponent  $\nu_\perp$  by plotting  $L^{\beta/\nu_\perp}\rho_s(\zeta, L)$  versus  $L^{1/\nu_\perp}\Delta$  for various system sizes, seeking the value of  $\nu_\perp$  which yields the best data collapse. Figure 6 shows that a good collapse is obtained using  $1/\nu_\perp = 0.704(5)$ . The critical exponent  $\beta$  that relates the order parameter  $\rho_s$  with  $\Delta$  through the relation  $\rho_s = \Delta^\beta$  is then easily determined as  $\beta = 0.322(5)$ .

Table I compares our estimates for critical exponents with those obtained in studies of other one-dimensional models in the CDP universality class. Despite apparent differences, it is important to recall that previous studies have revealed

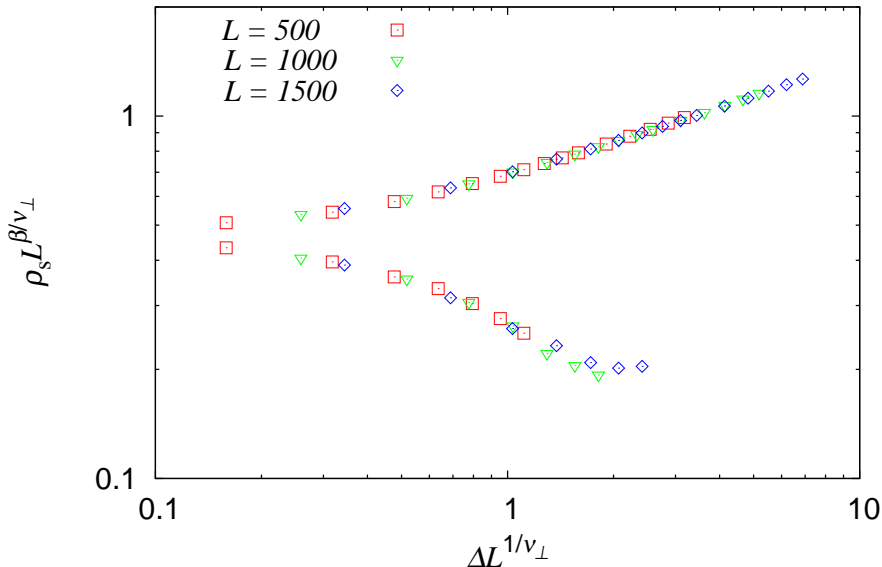


FIG. 6: Scaling plot for the density of active sites.

TABLE I: Critical exponents for one-dimensional models in the CDP universality class compared with estimates from present work. <sup>a</sup> Restricted Manna model [28]; <sup>b</sup> CDP Field theory [29]; <sup>c</sup> Sleepy Random Walkers [30].

Model	$\beta/\nu_\perp$	$z$	$\beta$
Rest. Manna <sup>a</sup>	0.213(6)	1.55(3)	0.29(1)
CDP - FT <sup>b</sup>	0.214(8)	1.47(4)	0.28(2)
SRW <sup>c</sup>	0.212(6)	1.50(4)	0.290(4)
Present work	0.227(5)	1.44(3)	0.322(5)

that simulations of large systems (20 000 sites or larger) are needed to obtain reliable values of critical exponents for this class [28, 30].

## V. CONCLUSIONS

We study a height-restricted fixed-density version of the Oslo sandpile in one dimension. At each site, the limiting height  $z_c$  may be either 2 or 3. The model is found to exhibit a continuous phase transition between an active and an absorbing state at a critical value of the particle density,  $\zeta_c$ . The one-site mean-field approximation predicts  $\zeta_c = 1$ , whereas simulations yield  $\zeta_c = 1.6400(2)$ . The small sizes

analyzed here limit the reliability of our estimates for the critical exponents. Given the comparison with the literature values shown in Table II, a tentative conclusion that the restricted Oslo model belongs to the conserved directed percolation class seems reasonable. More definitive conclusions will require studies of larger systems.

- 
- [1] P. Bak, C. Tang, and K. Wiesenfeld, Phys. Rev. Lett. **59**, 381 (1987).
  - [2] D. Dhar, Physica A **263**, 4 (1999).
  - [3] R. Dickman, M. A. Muñoz, A. Vespignani, and S. Zapperi, Braz. J. Phys. **30**, 27 (2000).
  - [4] M. A. Muñoz, R. Dickman, R. Pastor-Satorras, A. Vespignani, and S. Zapperi, *in Modeling Complex Systems* (edited by J. Marro and P. L. Garrido, AIP Conf. Proc. 574 (AIP, Melville, NY, 2001)), Phys. A **306**, 90 (2002).
  - [5] R. Dickman, Physica A **306**, 90 (2002).
  - [6] G. Grinstein, *in Scale Invariance, Interfaces and Nonequilibrium Dynamics*, Vol. **366** of NATO Advanced Study Institute, Series B: Physics (edited by A. McKane et al. (Plenum), New York, 1995).
  - [7] C. Tang and P. Bak, Phys. Rev. Lett. **60**, 2347 (1988).
  - [8] A. Vespignani and S. Zapperi, Phys. Rev. Lett. **78**, 4793 (1997).
  - [9] A. Vespignani and S. Zapperi, Phys. Rev. E **57**, 6345 (1998).
  - [10] R. Dickman, A. Vespignani, and S. Zapperi, Phys. Rev. E **57**, 5095 (1998).
  - [11] A. Vespignani, R. Dickman, M. A. Muñoz, and Stefano Zapperi, Phys. Rev. Lett. **81**, 5676 (1998).
  - [12] M. A. Muñoz, R. Dickman, A. Vespignani, and Stefano Zapperi, Phys. Rev. E **59**, 6175 (1999).
  - [13] A. Chessa, E. Marinari, and A. Vespignani, Phys. Rev. Lett. **80**, 4217 (1998).
  - [14] A. Montakhab and J. M. Carlson, Phys. Rev. E **58**, 5608 (1998).
  - [15] S. S. Manna, J. Stat. Phys. **59**, 509 (1990).
  - [16] S. S. Manna, J. Phys. A **24**, L363 (1991).
  - [17] K. Christensen and N.R. Moloney, *Complexity and Criticality* (Imperial College Press,

- London, 2005).
- [18] R. Dickman, T. Tomé, and M. J. de Oliveira, Phys. Rev. E **66**, 016111 (2002).
  - [19] J. A. Bonachela and M. A. Muñoz, Phys. Rev. E **78**, 041102 (2008).
  - [20] R. Dickman, Phys. Rev. E **73**, 036131 (2006).
  - [21] S. D. da Cunha, R. R. Vidigal, L. R. da Silva, and R. Dickman, Eur. Phys. J. B **72**, 441 (2009).
  - [22] M. Basu et al., Phys. Rev. Lett. **109**, 015702 (2012).
  - [23] W. H. Press, Saul A. Teukolsky, William T. Vetterling, and Brian V. Flannery, *Numerical Recipes* (Cambridge University Press, New York, 2007).
  - [24] T. E. Harris, Ann. Probab. **2**, 969 (1974).
  - [25] J. Marro and R. Dickman, *Nonequilibrium Phase Transitions in Lattice Models* (Cambridge University Press, Cambridge, 1999).
  - [26] R. Dickman, W. M. Rabêlo, and G. Ódor, Phys. Rev. E **65**, 016118 (2002).
  - [27] P. Grassberger and A. de la Torre, Ann. Phys. (N.Y.) **122**, 373 (1999).
  - [28] R. Dickman, Phys. Rev. E **73**, 036131 (2006).
  - [29] J. J. Ramasco, M. A. Muñoz, and C. A. da Silva Santos, Phys. Rev. E **69**, 045105(R) (2004).
  - [30] J. C. Mansur Filho and R. Dickman, J. Stat. Mech. (2011) P05029.